Quantum logic operations on two distant atoms trapped in two optical-fibre-connected cavities

Zhang Ying-Qiao(张英俏)[a)b)†], Zhang Shou(张 寿)[a)],
Yeon Kyu-Hwang[b)], and Yu Seong-Cho[b)]

[a)] *Department of Physics, College of Science, Yanbian University, Yanji* 133002, *China*
[b)] *BK21 Physics Program and Department of Physics, College of Natural Sciences, Chungbuk National University, Cheongju, Chungbuk,* 361–763, *Republic of Korea*

(Received 18 April 2011; revised manuscript received 17 May 2011)

Based on the coupling of two distant three-level atoms in two separate optical cavities connected with two optical fibres, schemes on the generation of several two-qubit logic gates are discussed under the conditions of $\Delta = \delta - 2\nu\cos\pi k/2 \gg g/2$ and $\nu \sim g$. Discussion and analysis of the fidelity, gate time and experimental setups show that our schemes are feasible with current optical cavity, atomic trap and optical fibre techniques. Moreover, the atom–cavity–fibre coupling can be used to generate an N-qubit nonlocal entanglement and transfer quantum information among N distant atoms by arranging N atom–cavity assemblages in a line and connecting each two adjacent cavities with two optical fibres.

Keywords: quantum logic gate, cavity QED, optical fibre

PACS: 03.67.Lx, 42.50.Pq **DOI:** 10.1088/1674-1056/20/12/120310

1. Introduction

A practical quantum computer requires the manipulation of large-scale qubits. The increase of the number of involved qubits in the register not only induces an increasing destructive effects of decoherece[1] but also incurs some undesired interactions among the qubits of the same register.[2] In order to solve these problems, distributed quantum computing[3,4] is introduced. The distributed quantum computing can be performed in a quantum computation network that contains many spatially separated local processors and each processor operates on a small number of qubits. A prerequisite in constructing the distributed quantum computing is the quantum logic operations on distant qubits among these processors in a network. In recent years, a series of such quantum logic operations has been studied based on a linear optics element[5−8] and a coupled atom–cavity–fibre system.[9−15] Especially, the coherent coupling of two distant atoms trapped in two separate cavities connected by an optical fibre provides the extensive applications in various types of two-qubit logic gates. For example, Serafini *et al.*[9] investigated the two-qubit swap gate and the controlled-phase gate in a fibre-connected two-cavity system with one atom contained in each cavity under the regime of $\nu \gg g$. Then this scheme was generalized to implement quantum state transfer and logic gates with multiple atoms trapped in each cavity.[10] Substituting the two-level atoms in the scheme[9] with three-level atoms and considering the resonance coupling of the atoms, cavities and fibre mode, a two-qubit phase gate is proposed within the null- and single-excitation subspaces[11] beyond the limit $\nu \gg g$. Furthermore, the two-atom–two-cavity–fibre system also provides an alternative scheme to implement the two-qubit phase gate via adiabatic passage[12] and virtual excitation.[13] Recently, a scheme of arbitrarily controlling the coherent coupling dynamics of multiple atoms trapped in multiple cavities linked by optical fibres was proposed.[16] Based on this model, a quantum gate between any pair of qubits can be generated.

Here we propose the alternative schemes to generate a two-qubit phase gate, a swap gate and a CNOT gate on two distant three-level atoms trapped in two separate cavities connected with two optical fibres. Our work functions are in the regime of $\nu \sim g$, in this case the difficulty for experimental performance is largely lowered compared with schemes based on the limit of $\nu \gg g$. Based on the two-qubit operations, the present model can be easily generalized to

†Corresponding author. E-mail: yqzhang@ybu.edu.cn
© 2011 Chinese Physical Society and IOP Publishing Ltd

the generation of an N-qubit nonlocal entangled state and the transfer of a quantum state between N distant atoms by the design of arranging N atom–cavity assemblages in a line and connecting each two adjacent cavities with two optical fibres.

The remainder of the present paper is organized as follows. In Section 2 we describe the coupling dynamics for the atom–cavity–fibre system. In Sections 3–5 we introduce the processes for the generation of a two-qubit phase gate, swap gate and CNOT gate, respectively. In Section 6, as the applications of the present quantum gates, schemes of the generation of an N-qubit nonlocal entangled state and quantum state transfer between N distant atoms are introduced briefly. A discussion and conclusion are given in Section 7.

2. Coupling dynamics for two distant atoms trapped in two separate cavities connected via two optical fibres

Considering that two identical three-level atoms (Fig. 1) are trapped in two separate cavities (Fig. 2) connected by two optical fibres. Each atom has one excited state $|e\rangle_j$ and two ground states $|g\rangle_j$ and $|i\rangle_j$ ($j \in 1, 2$) and the level $|i\rangle_j$ is not involved in the interaction with the cavity mode. Transition $|e\rangle_j \leftrightarrow |g\rangle_j$ is coupled to the cavity mode with the coupling constant g_j and detuning δ. So the coupling of the two atoms and two cavity modes is given by the interaction Hamiltonian

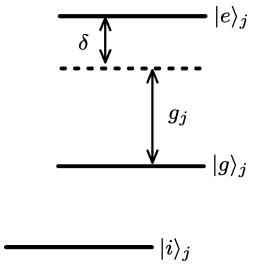


Fig. 1. Atomic configuration with three levels $|e\rangle_j$, $|g\rangle_j$, and $|i\rangle_j$. The transition $|e\rangle_j \leftrightarrow |g\rangle_j$ is coupled to the cavity mode with the coupling constant g_j and detuning δ.

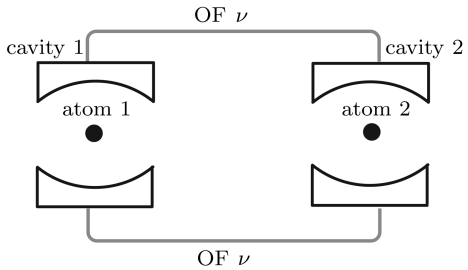


Fig. 2. Experimental setup for two atoms trapped in two distant cavities connected by two optical fibres (OF). ν is the coupling strength of the cavities to the optical fibres.

$$H_{\rm I} = (g_1 a_1 S_1^+ + g_2 a_2 S_2^+)\,{\rm e}^{{\rm i}\delta t} + {\rm H.c.}, \tag{1}$$

where $\delta = \omega_0 - \omega_c$ with ω_0 being the atomic transition frequency and ω_c the frequency of the two cavity modes a_1 and a_2. Atomic operators $S_j^+ = |e\rangle_j\langle g|$, $S_j^- = |g\rangle_j\langle e|$. In the short fibre limit,[9] the coupling of the cavity modes to the fibre modes is described by the interaction Hamiltonian

$$H_{\rm II} = \sum_{l=1}^{2} \nu b_l (a_1^\dagger + a_2^\dagger) + {\rm H.c.}, \tag{2}$$

where b_l ($l \in 1, 2$) is the annihilation operator of the two fibre modes and ν is the coupling constant of the cavity mode to the fibre mode. Actually, the coupling constant ν can be adjusted by changing the reflectivity of the cavity mirror connected to the fibre.[9] Defining four bosonic modes[16]

$$\begin{aligned} C_1 &= \frac{1}{2}(-{\rm i}a_1 - b_1 + {\rm i}a_2 + b_2), \\ C_2 &= \frac{1}{2}(-a_1 + b_1 - a_2 + b_2), \\ C_3 &= \frac{1}{2}({\rm i}a_1 - b_1 - {\rm i}a_2 + b_2), \\ C_4 &= \frac{1}{2}(a_1 + b_1 + a_2 + b_2), \end{aligned} \tag{3}$$

the Hamiltonian that describes atom–cavity coupling and cavity–fibre coupling can be rewritten as

$$H_{\rm I}' = \sum_{k=1}^{4} \left(\frac{g_1}{2} S_1^+ {\rm e}^{{\rm i}k\pi/2} + \frac{g_2}{2} S_2^+ {\rm e}^{{\rm i}3k\pi/2}\right) C_k\, {\rm e}^{{\rm i}\delta t} + {\rm H.c.}, \tag{4}$$

and

$$H_{\rm II}' = 2\nu \sum_{k=1}^{4} \cos\frac{\pi k}{2} C_k^\dagger C_k, \tag{5}$$

respectively. Now, by performing the transformation ${\rm e}^{{\rm i}H_{\rm II}' t} H_{\rm I}' {\rm e}^{-{\rm i}H_{\rm II}' t}$ leads to

$$H_{\rm I}'' = \sum_{k=1}^{4} \left(\frac{g_1}{2} S_1^+ {\rm e}^{{\rm i}k\pi/2} + \frac{g_2}{2} S_2^+ {\rm e}^{{\rm i}3k\pi/2}\right) C_k\, {\rm e}^{{\rm i}\Delta t} + {\rm H.c.}, \tag{6}$$

where $\Delta = \delta - 2\nu\cos(\pi k/2)$. Under the condition of $\Delta \gg g_1/2$, $g_2/2$, atoms do not exchange energy with

cavity modes and fibre modes, so the effective Hamiltonian can be expressed as

$$\begin{aligned} H_{\rm eff} &= \sum_{k=1}^{4}\frac{1}{4\Delta}(g_1^2|e\rangle_1\langle e| + g_2^2|e\rangle_2\langle e|)C_kC_k^\dagger \\ &\quad -\sum_{k=1}^{4}\frac{1}{4\Delta}(g_1^2|g\rangle_1\langle g| + g_2^2|g\rangle_2\langle g|)C_k^\dagger C_k \\ &\quad +\sum_{k=1}^{4}\frac{g_1g_2}{4\Delta}(S_1^+S_2^-\,{\rm e}^{-{\rm i}k\pi} + S_1^-S_2^+\,{\rm e}^{{\rm i}k\pi}). \end{aligned} \tag{7}$$

We note that the four normal modes C_k ($k \in 1,2,3,4$) interact with the atoms, owing to the existence of the cavity fields, though they are not coupled with each other. To obtain the reduced dynamics of the system, we assume that two cavity modes and two fibre modes are all initially in the vacuum states. Therefore the effective Hamiltonian $H_{\rm eff}$ becomes

$$\begin{aligned} H'_{\rm eff} &= \sum_{k=1}^{4}\frac{1}{4\Delta}(g_1^2|e\rangle_1\langle e| + g_2^2|e\rangle_2\langle e|) \\ &\quad +\sum_{k=1}^{4}\frac{g_1g_2}{4\Delta}(S_1^+S_2^-\,{\rm e}^{-{\rm i}k\pi} + S_1^-S_2^+\,{\rm e}^{{\rm i}k\pi}). \end{aligned} \tag{8}$$

For simplicity, we suppose that $g_1 = g_2 = g$ hereafter, and the Hamiltonian $H'_{\rm eff}$ becomes

$$\begin{aligned} H''_{\rm eff} &= (\lambda_1-\lambda)(|e\rangle_1\langle e| + |e\rangle_2\langle e|) \\ &\quad +\lambda(S_1^+S_2^- + S_1^-S_2^+), \end{aligned} \tag{9}$$

where

$$\lambda = \frac{2g^2\nu^2}{\delta(\delta^2-4\nu^2)}, \quad \lambda_1 = \frac{g^2\delta^2}{\delta(\delta^2-4\nu^2)}. \tag{10}$$

Combining the constraint condition $\Delta = \delta - 2\nu\cos(\pi k/2) \gg g/2$ with Eq. (10), we have $\lambda_1 \gg 2\lambda$.

3. Phase gate

In order to generate a two-qubit phase gate, quantum information is encoded in the basis $\{|e\rangle_1, |g\rangle_1, |g\rangle_2, |i\rangle_2\}$. Based on the Schrödinger equation ($\hbar = 1$)

$${\rm i}\frac{\partial}{\partial t}|\Psi(t)\rangle = H''_{\rm eff}|\Psi(t)\rangle, \tag{11}$$

different initial states $|eg\rangle$, $|ei\rangle$, $|gg\rangle$, and $|gi\rangle$ of the two atoms, respectively, evolve into

$$\begin{aligned} &|eg\rangle \to a(t)|eg\rangle + b(t)|ge\rangle \quad |ei\rangle \to c(t)|ei\rangle, \\ &|gg\rangle \to |gg\rangle, \quad |gi\rangle \to |gi\rangle, \end{aligned} \tag{12}$$

where

$$\begin{aligned} a(t) &= \frac{1}{2}\{\cos(2\lambda-\lambda_1)t + {\rm i}\sin(2\lambda-\lambda_1)t \\ &\quad + \cos\lambda_1 t - {\rm i}\sin\lambda_1 t\}, \\ b(t) &= \frac{1}{2}\{-\cos(2\lambda-\lambda_1)t - {\rm i}\sin(2\lambda-\lambda_1)t \\ &\quad + \cos\lambda_1 t - {\rm i}\sin\lambda_1 t\}, \\ c(t) &= \cos(\lambda_1-\lambda)t - {\rm i}\sin(\lambda_1-\lambda)t. \end{aligned} \tag{13}$$

We have

$$a(t) = 1, \quad b(t) = 0, \quad c(t) = -1, \tag{14}$$

if the parameters λ_1 and λ satisfy the conditions $\lambda_1 t = 2n\pi$ ($n = 1,2,3,\ldots$) and $\lambda t = (2m+1)\pi$ ($m = 0,1,2,3,\ldots$). So far, we have obtained a two-qubit phase gate as

$$\begin{aligned} &|eg\rangle \to |eg\rangle, \quad |ei\rangle \to -|ei\rangle, \\ &|gg\rangle \to |gg\rangle, \quad |gi\rangle \to |gi\rangle. \end{aligned} \tag{15}$$

Based on Eq. (12), we can prepare a two-qubit entangled state from the initial state $|\psi_0\rangle = (|e\rangle_1 + |g\rangle_1)/\sqrt{2} \otimes (|g\rangle_2 + |i\rangle_2)/\sqrt{2}$ as

$$\begin{aligned} |\psi_{\rm e}\rangle &= \frac{1}{(\sqrt{2})^2}\{a(t)|eg\rangle + b(t)|ge\rangle + c(t)|ei\rangle \\ &\quad + |gg\rangle + |gi\rangle\}_{12}. \end{aligned} \tag{16}$$

The fidelity $F_{\rm p} = |\langle\psi_i|\psi_e\rangle|^2$ is obtainable based on the ideal entangled state $|\psi_{\rm i}\rangle = \{|e\rangle_1(|g\rangle_2 - |i\rangle_2) + |g\rangle_1(|g\rangle_2 + |i\rangle_2)\}/(\sqrt{2})^2$ induced by Eq. (15). We have plotted $F_{\rm p}$ curves each as a function of λ_1/λ under the conditions of $m = 0$ and $m = 1$, respectively, in Figs. 3(a) and 3(b). According to Figs. 3(a) and 3(b), fidelity oscillates from the minimal value 0 to maximal value 1 periodically accompanied with the changing of λ_1/λ. A comparison of Figs. 3(a) and 3(b) shows that the oscillating period decreases with the increase of m.

The computation on $F_{\rm p}$ for different values of m and λ_1/λ shows that

$$\begin{cases} F_{\rm p} = 1, & \text{if} \quad (2m+1)\dfrac{\lambda_1}{\lambda} = 2n, \\ F_{\rm p} = 0, & \text{if} \quad (2m+1)\dfrac{\lambda_1}{\lambda} = 2n+1, \\ 0 < F_{\rm p} < 1, & \text{if} \quad (2m+1)\dfrac{\lambda_1}{\lambda} = \text{other values}, \end{cases} \tag{17}$$

where $n \gg 2m+1$ according to $\lambda_1 \gg 2\lambda$. That is to say, in order to generate a two-qubit phase gate with a high fidelity, choosing an even number $(2m+1)\lambda_1/\lambda$ is suitable.

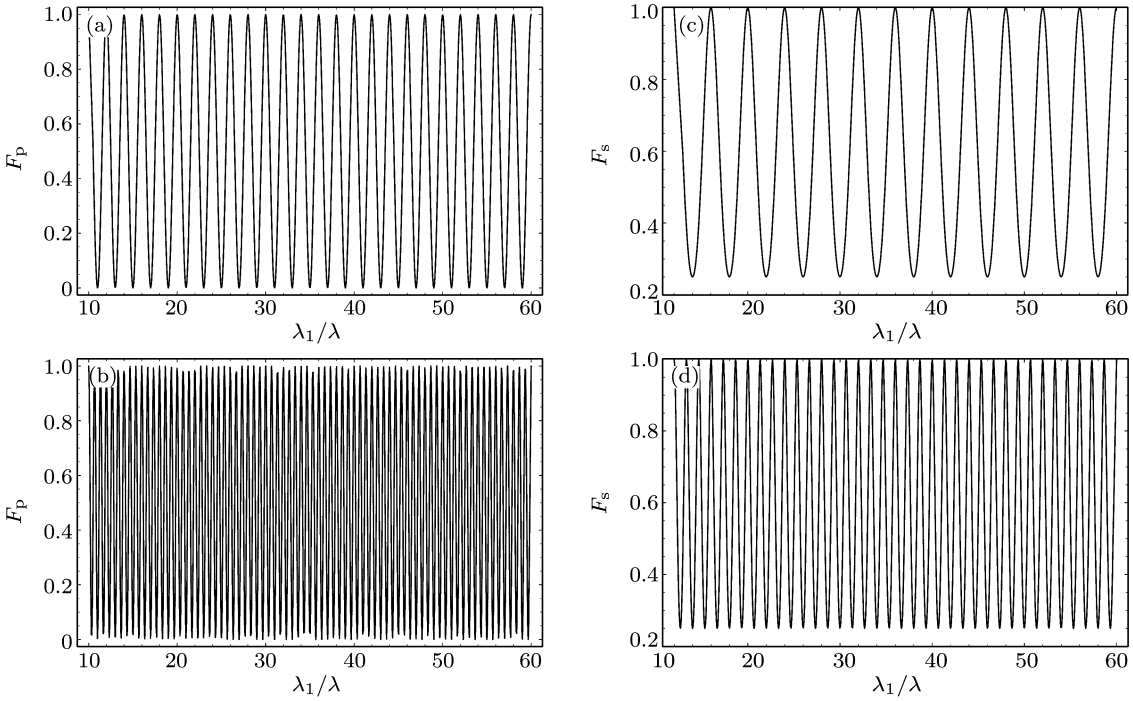


Fig. 3. Curves of the phase gate fidelity F_p and the swap gate fidelity F_s versus the continuous ratio λ_1/λ for $m = 0$ (panels (a) and (c)), and $m = 1$ (panels (b) and (d)).

4. Swap gate

For the generation of a swap gate, quantum information is encoded in the basis $\{|e\rangle_1, |g\rangle_1, |e\rangle_2, |g\rangle_2\}$. Based on the Schrödinger equation in Eq. (11), the evolutions of different initial states $|eg\rangle$, $|ge\rangle$, $|ee\rangle$, and $|gg\rangle$ are

$$\begin{aligned} &|eg\rangle \to a(t)|eg\rangle + b(t)|ge\rangle, \\ &|ge\rangle \to a(t)|ge\rangle + b(t)|eg\rangle, \\ &|ee\rangle \to d(t)|ee\rangle, \quad |gg\rangle \to |gg\rangle, \end{aligned} \tag{18}$$

where

$$d(t) = \cos 2(\lambda_1 - \lambda)t - \mathrm{i} \sin 2(\lambda_1 - \lambda)t. \tag{19}$$

When $\lambda_1 t = 2n\pi$ $(n = 1, 2, 3, \ldots)$, $\lambda t = (2m + 1)\pi/2$ $(m = 0, 1, 2, 3, \ldots)$, we have

$$a(t) = 0, \quad b(t) = 1, \quad d(t) = -1. \tag{20}$$

Thus

$$\begin{aligned} &|eg\rangle \to |ge\rangle, \quad |ge\rangle \to |eg\rangle, \\ &|ee\rangle \to -|ee\rangle, \quad |gg\rangle \to |gg\rangle. \end{aligned} \tag{21}$$

Then using a classical field to drive the transition $|e\rangle \to |i\rangle$ on atom 2, we have

$$\begin{aligned} &|ge\rangle \to |gi\rangle, \quad |eg\rangle \to |eg\rangle, \\ &-|ee\rangle \to -|ei\rangle, \quad |gg\rangle \to |gg\rangle. \end{aligned} \tag{22}$$

Next, performing the phase operation described in Eq. (15) on the two atoms, the states become

$$\begin{aligned} &|gi\rangle \to |gi\rangle, \quad |eg\rangle \to |eg\rangle, \\ &-|ei\rangle \to |ei\rangle, \quad |gg\rangle \to |gg\rangle. \end{aligned} \tag{23}$$

Finally, using a classical field to drive the transition $|i\rangle \to |e\rangle$ on atom 2, we have

$$\begin{aligned} &|gi\rangle \to |ge\rangle, \quad |eg\rangle \to |eg\rangle, \\ &|ei\rangle \to |ee\rangle, \quad |gg\rangle \to |gg\rangle. \end{aligned} \tag{24}$$

Therefore, we have obtained a swap gate

$$\begin{aligned} &|eg\rangle \to |ge\rangle, \quad |ge\rangle \to |eg\rangle, \\ &|ee\rangle \to |ee\rangle, \quad |gg\rangle \to |gg\rangle. \end{aligned} \tag{25}$$

Then we check how well the swap gate works. Suppose that the initial state of the two atoms are in $|\psi_{0s}\rangle = (\alpha_1|e\rangle_1 + \beta_1|g\rangle_1) \otimes (\alpha_2|e\rangle_2 + \beta_2|g\rangle_2)$. According to the evolution in Eq. (18), we can obtain a result state as

$$\begin{aligned} &|\psi_{es}\rangle \\ &= \alpha_1\alpha_2 \mathrm{d}(t)|ee\rangle_{12} + \{\alpha_1\beta_2 a(t) + \beta_1\alpha_2 b(t)\}|eg\rangle_{12} \\ &\quad + \{\alpha_1\beta_2 b(t) + \beta_1\alpha_2 a(t)\}|ge\rangle_{12} + \beta_1\beta_2|gg\rangle_{12}. \end{aligned} \tag{26}$$

The average fidelity

$$F_s = \int_0^{2\pi} \mathrm{d}\vartheta_1 \int_0^{2\pi} \mathrm{d}\vartheta_2 |\langle\psi_{is}|\psi_{es}\rangle|^2/4\pi^2$$

can be obtained based on the ideal result state $|\psi_{\rm is}\rangle$. The curves of $F_{\rm s}$ versus λ_1/λ are plotted for $m = 0$ and $m = 1$, respectively, in Figs. 3(c) and 3(d). From Figs. 3(c) and 3(d), the values for $F_{\rm s}$ take on periodic oscillations from the minimal value 0.25 to maximal value 1 with the changing of λ_1/λ. The oscillating periodic decreases with the increase of m.

The values for $F_{\rm s}$ can be described as

$$\begin{cases} F_{\rm s} = 1, & \text{if} \quad (2m+1)\dfrac{\lambda_1}{\lambda} = 4n, \\ F_{\rm s} = 0.25, & \text{if} \quad (2m+1)\dfrac{\lambda_1}{\lambda} = \text{even numbers, except } 4n, \\ 0.25 < F_{\rm s} < 1, & \text{if} \quad (2m+1)\dfrac{\lambda_1}{\lambda} = \text{other values}, \end{cases} \tag{27}$$

with $2n \gg 2m+1$ according to $\lambda_1 \gg 2\lambda$. Apparently, for a high fidelity, the value for $(2m+1)\lambda_1/\lambda$ to take $4n$ is ideal. Due to the fact that the phase operation has been applied to the generation of the swap gate, the total fidelity of the swap gate is $F_{\rm s} * F_{\rm p}$.

5. CNOT gate

In this section, we discuss the generation of a CNOT gate based on the phase gate. Firstly, performing the following H operation

$$\begin{aligned} |g\rangle &\to \frac{1}{\sqrt{2}}(|g\rangle + |i\rangle), \\ |i\rangle &\to \frac{1}{\sqrt{2}}(|g\rangle - |i\rangle), \end{aligned} \tag{28}$$

on atom 2 of the initial states $|eg\rangle$, $|ei\rangle$, $|gg\rangle$, and $|gi\rangle$ leads to

$$\begin{aligned} |eg\rangle &\to \frac{1}{\sqrt{2}}(|eg\rangle + |ei\rangle), \\ |ei\rangle &\to \frac{1}{\sqrt{2}}(|eg\rangle - |ei\rangle), \\ |gg\rangle &\to \frac{1}{\sqrt{2}}(|gg\rangle + |gi\rangle), \\ |gi\rangle &\to \frac{1}{\sqrt{2}}(|gg\rangle - |gi\rangle). \end{aligned} \tag{29}$$

Then the phase operation in Eq. (15) is performed on the two atoms, which leads to

$$\begin{aligned} \frac{1}{\sqrt{2}}(|eg\rangle + |ei\rangle) &\to \frac{1}{\sqrt{2}}(|eg\rangle - |ei\rangle), \\ \frac{1}{\sqrt{2}}(|eg\rangle - |ei\rangle) &\to \frac{1}{\sqrt{2}}(|eg\rangle + |ei\rangle), \\ \frac{1}{\sqrt{2}}(|gg\rangle + |gi\rangle) &\to \frac{1}{\sqrt{2}}(|gg\rangle + |gi\rangle), \\ \frac{1}{\sqrt{2}}(|gg\rangle - |gi\rangle) &\to \frac{1}{\sqrt{2}}(|gg\rangle - |gi\rangle). \end{aligned} \tag{30}$$

Next, another H operation on atom 2 results in the final states

$$\begin{aligned} \frac{1}{\sqrt{2}}(|eg\rangle - |ei\rangle) &\to |ei\rangle, \\ \frac{1}{\sqrt{2}}(|eg\rangle + |ei\rangle) &\to |eg\rangle, \\ \frac{1}{\sqrt{2}}(|gg\rangle + |gi\rangle) &\to |gg\rangle, \\ \frac{1}{\sqrt{2}}(|gg\rangle - |gi\rangle) &\to |gi\rangle. \end{aligned} \tag{31}$$

Therefore, we have obtained a CNOT gate

$$\begin{aligned} |eg\rangle \to |ei\rangle, \quad |ei\rangle \to |eg\rangle, \\ |gg\rangle \to |gg\rangle, \quad |gi\rangle \to |gi\rangle. \end{aligned} \tag{32}$$

6. Other applications

The coherence dynamics also offers the possibilities to entangle N distant atoms trapped in N separate cavities and transfer quantum information between N distant atoms based on N atom–cavity assemblages connected by $2(N-1)$ optical fibres (see Fig. 4). For the generation of an N-qubit entangled state, the initial states of the odd-th atoms are prepared in the state $(|e\rangle+|g\rangle)/\sqrt{2}$ and the even-th atoms are prepared in $(|g\rangle+|i\rangle)/\sqrt{2}$. Any two adjacent atoms can be entangled directly based on the evolution in Eq. (15). When the entanglement of two target adjacent atoms (κ, $\kappa+1$) is implemented, the coupling ν_κ between the relevant cavities (κ, $\kappa+1$) and optical fibres is open and the other fibre–cavity couplings ν_ℓ ($\ell = 1, 2, \ldots, N-1), (\ell \neq \kappa)$ are closed using the optical switches. The N-atom entanglement can be constructed step by step by entangling two adjacent atoms in the order of atoms (1, 2), atoms (2, 3), atoms (3, 4), …, atoms ($(N-1)$, N). By doing so, we can entangle N nonlocal atoms trapped in N distant cavities connected with $2(N-1)$ optical fibres. To transfer

quantum information from the 1-st atom to a distant N-th atom, the initial states for the 1-st atom is in the state $\alpha|e\rangle+\beta|g\rangle$ and the remaining $(N-1)$ atoms are all in state $|g\rangle$. The quantum state in atom 1 can be transferred easily to atom 2 based on the evolution described in Eq. (25). Repeating this process, quantum state $\alpha|e\rangle+\beta|g\rangle$ can be transferred orderly from atom 2 to atom 3, and from atom 3 to atom 4, ..., from atom $(N-1)$ to atom N. When quantum state transfer occurs between two target adjacent atoms (κ, κ+1), apart from the relevant coupling ν_κ between the cavities (κ, κ+1) and the optical fibres, the remaining fibre–cavity couplings ν_ℓ $(\ell=1,2,\ldots,N-1),(\ell\neq\kappa)$ must be shut off using the optical switches.

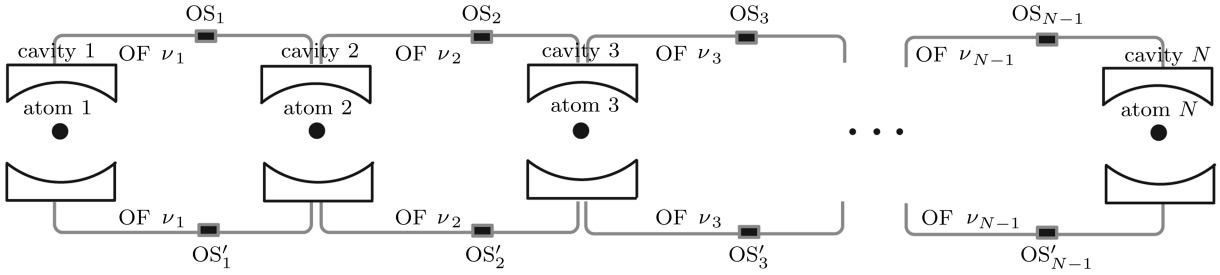


Fig. 4. Experimental setup for implementation of N-qubit entanglement and quantum information transfer by arranging N cavities in a line and connecting each two-adjacent cavities with two optical fibres (OF). The small rectangles represent optical switches (OS) that control whether there is interaction between two adjacent cavities. ν_κ is the coupling strength of the cavities (κ, $\kappa+1$) with the optical fibres.

7. Discussion and conclusion

In this work, we mainly discuss the generation of a two-qubit phase gate, swap gate and CNOT gate. In the generation process, the constraint condition $\Delta=\delta-2\nu\cos(\pi k/2)\gg g/2$ that offers the required coupling mechanism of the cavities to atoms and optical fibres must be satisfied, and which induces the relation $\lambda_1\gg 2\lambda$. However, too large ratio of λ_1/λ will increase the gate time and be not advantageous to perform the high efficient quantum computation. Setting $\lambda_1=50\lambda$ is compatible to both the constraint condition and the gate time. Together with setting $m=0$, $\nu=g$, and $g/2\pi=86$ MHz,[17] the phase gate time is $t_{\rm p}=\pi/\lambda=2.79$ μs and the swap gate time $t_{\rm s}$ is the sum of the evolution time $t_{\rm e}=\pi/2\lambda$ and the phase gate time $t_{\rm p}$, i.e., $t_{\rm s}=t_{\rm e}+t_{\rm p}=3\pi/2\lambda$. It should be noted that for the accomplishment of the swap gate, classical fields are used to perform the single-atom unitary transformations. The time for the single-atom operations can be suppressed to be an extremely short amount by choosing the classical fields with sufficiently strong intensity. Hence, the classical fields time is negligible in the total gate time. For the same reasons, the CNOT gate time is considered to be equivalent to phase gate time $t_{\rm p}$ though classical fields are necessary to perform H operation.

Then we discuss the experimental setups briefly. For the schemes under consideration, atoms with three levels including one excited state $|e\rangle$ and two ground states $|g\rangle$ and $|i\rangle$ are employed. The level $|i\rangle$ does not participate in the interaction with the cavity mode, but it is useful to encode the quantum information. The atomic configuration can be realized in cesium atom with the hyperfine levels $6{\rm P}_{3/2}F'=5$, $6{\rm S}_{1/2}F=4$, and $6{\rm S}_{1/2}F=3$[18] corresponding to three levels $|e\rangle$, $|g\rangle$, and $|i\rangle$, respectively.[11] In addition to atoms, atom–cavity coupling is also dependent on matched optical cavity. Fundamentally, several parameters to evaluate the capability of the optical cavity include cavity mode volume, cavity quality factor (high quality factor means low cavity loss) and fabrication, which makes whispering-gallery-mode (WGM) cavity[19,20,21] an ideal candidate in experiments superior to or compared favourably with other cavities, such as Fabry–Perot (FP) cavity and photonic bandgap (PBG) cavity.[17] It has been reported that the WGM cavity not only achieves ultrahigh-quality factor exceeding 10^8 while simultaneously obtaining a large coupling rate between the cavity and a cesium atom, but also has significant advantages in fabrication reproducibility, control and mode structure. According to Ref. [17], the toroidal cavity at a wavelength of 852 nm is suited for strong-coupling cavity QED with atomic cesium and the modest atom–cavity coupling can be obtained solely by adjusting the cavity diameter. In experiments, the WGM cavity is constructed by a toroid-shape silica disk with an underly silicon support pillar. The process for producing the toroid-shape microresonator on a microelectronic chip includes photolithography, pattern transfer into the silicon dioxide layer, selective dry etch

of the exposed silicon and selective reflow of the patterned silica, which has been demonstrated detailedly in Ref. [22].

For the fibres coupled to the cavities, near-lossless coupling between the fibres and the cavities is desirable and fundamental to the high-efficient and reliable quantum process in fibre-coupled cavity QED system. Tapered fibres[23] have been shown to provide a high coupling efficiency to cavities and are considered as an excellent coupling interface. According to Ref. [23] typical fibre tapers are 1 μm–4 μm-diameter air-clad silica cylinders and are fabricated by flame heating and pulling standard single-mode fibre into a narrow thread as shown in Refs. [24] and [25]. The fact that the coupling efficiency for tapered fibres to high-Q silica microspheres is in excess of 99.97% over FP and PBG cavities (97%) proves to be an ideal choice for connecting WGM cavities with tapered fibres.[17] Therefore, the combination of the cesium atoms, WGM cavities and tapered fibres in a fibre-coupled cavity QED system is an optimal selection for the physical realization of the present schemes with a high efficiency.

In conclusion, schemes for the generation of a two-qubit phase gate, swap gate and CNOT gate are proposed with two distant atoms trapped in two optical-fibre-connected cavities under the conditions of $\Delta = \delta - 2\nu\cos\pi k/2 \gg g/2$ and $\nu \sim g$. In the operation process, cavity modes and optical fibre modes are almost in vacuum states, thus the fidelity is insensitive to the decay of the cavity mode and fibre mode. Atomic level transition is between the ground state $6S_{1/2}F = 4$ and the excited state $6P_{3/2}F' = 5$, and a very small transverse decay rate for $6P_{3/2}$ state is achievable with current experiment technique, thus the effect of the transverse decay can be largely reduced. Discussion and analysis of the fidelity, generation time and experimental setups show that the present schemes are feasible with current optical cavity, atomic trap and optical fibre techniques. Moreover, the coherent coupling of the atoms, cavities and optical fibres can be used to generate an N-qubit nonlocal entangled state and transfer quantum information between N distant atoms by arranging N atom–cavity assemblages in a line and connecting each two adjacent cavities with two optical fibres.

References

[1] Palma G M, Suominen K A and Ekert A K 1996 *Proc. R. Soc. Lond.* A **452** 567

[2] DiVincenzo D P and Loss D 1998 *Superlattice Microstruc.* **23** 419

[3] Cirac J I, Ekert A K, Huelga S F and Macchiavello C 1999 *Phys. Rev.* A **59** 4249

[4] Paternostro M, Kim M S and Palma G M 2003 *J. Mod. Opt.* **50** 2075

[5] Xia Y, Song J and Song H S 2008 *Chin. Phys. Lett.* **25** 3150

[6] Song J, Xia Y and Song H S 2009 *Europhys. Lett.* **87** 50005

[7] Lin L H 2009 *Chin. Phys.* B **18** 1867

[8] Xia Y, Song J, Lu P M and Song H S 2011 *J. Phys.* B*: At. Mol. Opt. Phys.* **44** 025503

[9] Serafini A, Mancini S and Bose S 2006 *Phys. Rev. Lett.* **96** 010503

[10] Yin Z Q and Li F L 2007 *Phys. Rev.* A **75** 012324

[11] Yang Z B, Wu H Z, Su W J and Zheng S B 2009 *Phys. Rev.* A **80** 012305

[12] Ye S Y and Zheng S B 2008 *Opt. Commun.* **281** 1306

[13] Zheng S B 2009 *Appl. Phys. Lett.* **94** 154101

[14] Li Y L, Fang M F and Zeng K 2010 *Chin. Phys.* B **19** 010307

[15] Zheng S B 2010 *Chin. Phys.* B **19** 064204

[16] Zheng S B, Yang C P and Nori F 2010 *Phys. Rev.* A **82** 042327

[17] Spillane S M, Kippenberg T J, Vahala K J, Goh K W, Wilcut E and Kimble H J 2005 *Phys. Rev.* A **71** 013817

[18] Boca A, Miller R, Birnbaum K M, Boozer A D, McKeever J and Kimble H J 2004 *Phys. Rev. Lett.* **93** 233603

[19] Braginsky V B, Gorodetsky M L and Ilchenko V S 1989 *Phys. Lett.* A **137** 393

[20] Gorodetsky M L, Savchenkov A A and Ilchenko V S 1996 *Opt. Lett.* **21** 453

[21] Vernooy D W, Ilchenko V S, Mabuchi H, Streed E W and Kimble H J 1998 *Opt. Lett.* **23** 247

[22] Armani D K, Kippenberg T J, Spillane S M and Vahala K J 2003 *Nature* **421** 925

[23] Spillane S M, Kippenberg T J, Painter O J and Vahala K J 2003 *Phys. Rev. Lett.* **91** 043902

[24] Knight J C, Cheung G, Jacques F and Birks T A 1997 *Opt. Lett.* **22** 1129

[25] Cai M, Painter O and Vahala K J 2000 *Phys. Rev. Lett.* **85** 74